Electronic Supplementary Material (ESI) for Journal of Materials Chemistry C.

Supporting Information

Effect of Cation Arrangement on the Polaron Formation and Colossal Permittivity in $NiNb_2O_6$

Jian Wang[a,b], *Dandan Gao*[a], *Huan Liu*[a], *Jiyang Xie*[a], *Wanbiao Hu*[a,b]*

[a] Key Laboratory of LCR Materials and Devices of Yunnan Province, International Joint Research Center for Optoelectronic and Energy Materials, School of Materials and Energy, Yunnan University, Kunming 650091, P. R. China

[b] School of Physics and Astronomy, Yunnan University, Kunming 650091, P. R. China

* Corresponding authors: Wanbiao Hu (huwanbiao@ynu.edu.cn)

Keywords: disorder, electronic states, dielectric response, $NiNb_2O_6$ polymorphs, electron paramagnetic resonance

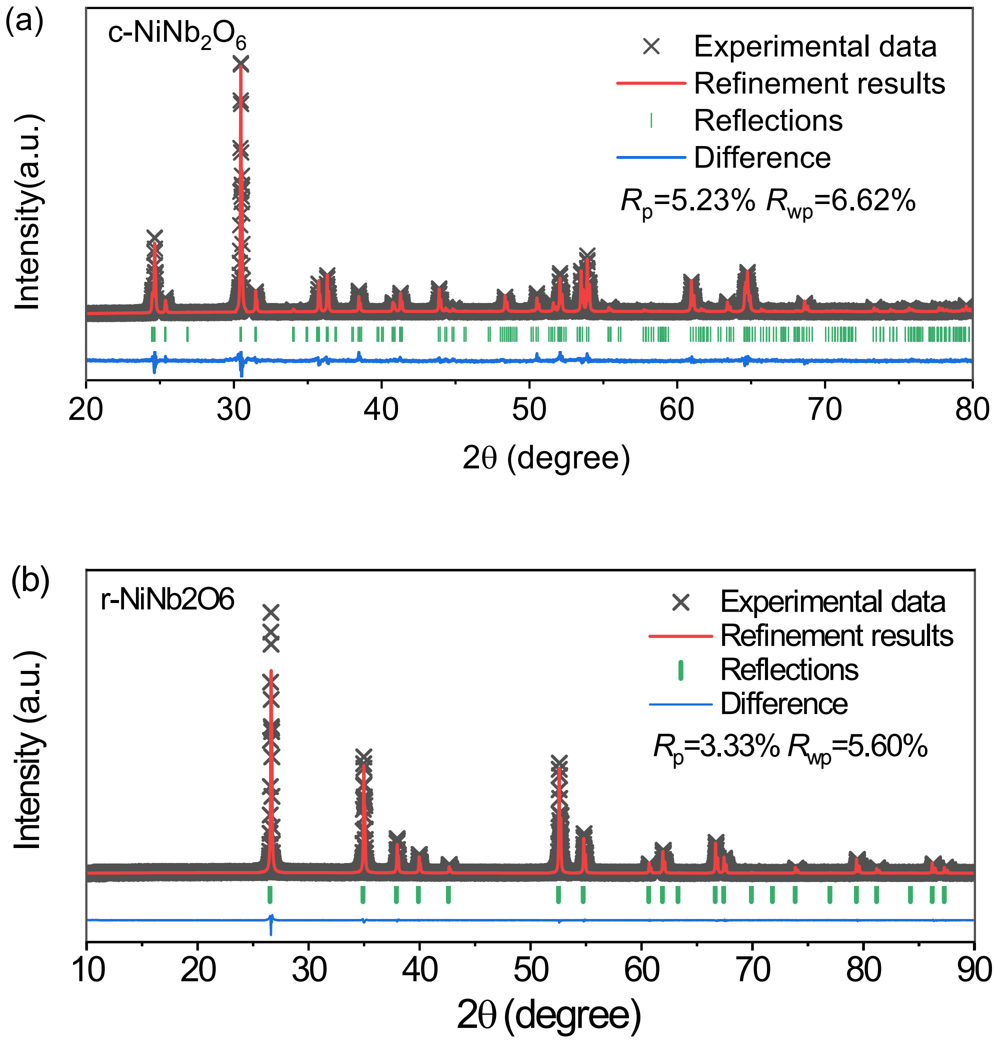

Figure S1 Rietveld refinement for the XRD patterns of (a) c-$NiNb_2O_6$ and (b) r-$NiNb_2O_6$. The results reveal the single phase of columbite and rutile structure for c-$NiNb_2O_6$ and r-$NiNb_2O_6$, respectively.

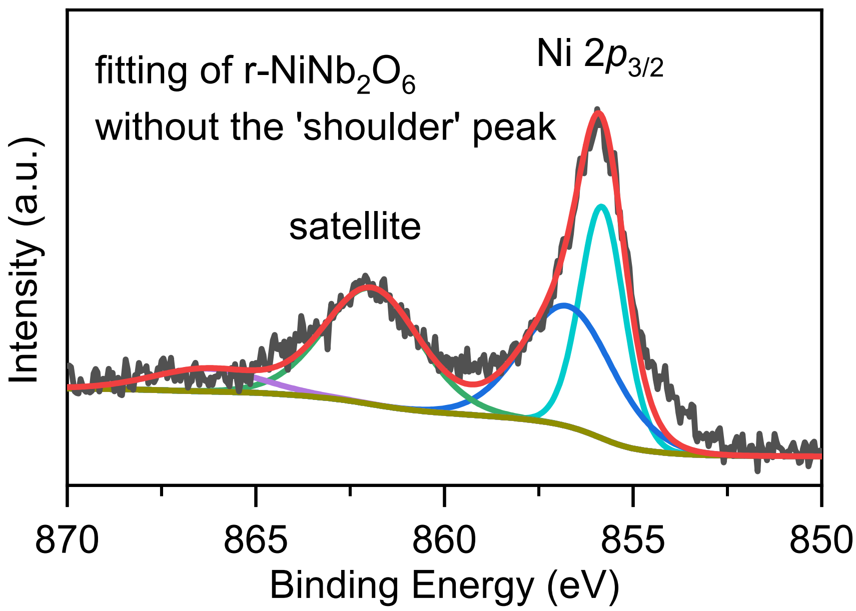

Figure S2 Illustration of the fitting results of the Ni 2*p* profile of r-$NiNb_2O_6$ with Ni^{2+}-only peaks. The deviation of the fitted curve from experimental data suggests that an extra peak by the lower energy side of Ni 2$p_{3/2}$ main peak is required for fitting.

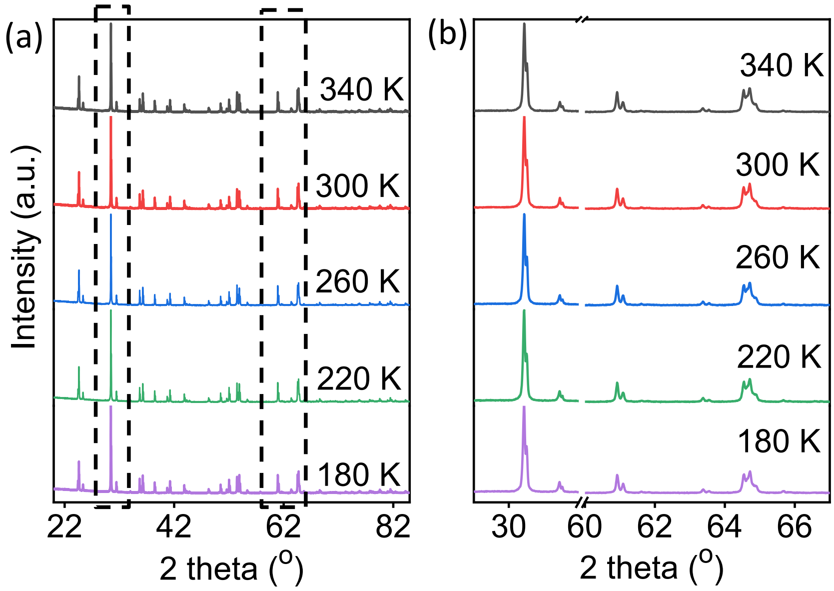

Figure S3 (a) XRD patterns for c-$NiNb_2O_6$ at 180 K < T < 340 K. (b) The enlarged areas as indicated by dashed rectangles in (a). The temperature in situ XRD results reveal no phase transition, thus the dielectric anomaly in this temperature range is considered in terms of long-range electron conduction.

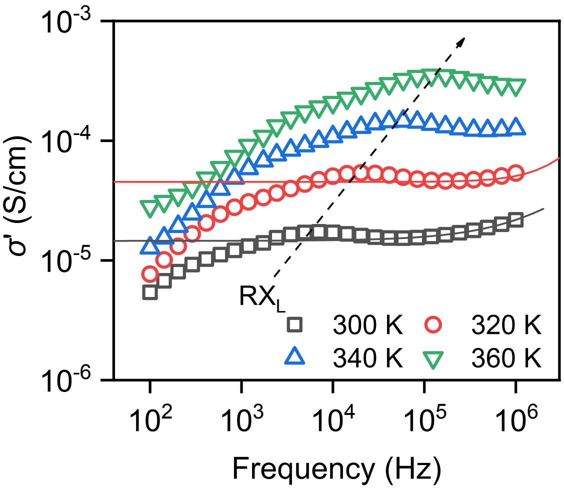

Figure S4 Frequency dependent ac conductivity σ' curves at 300 K ~ 360 K for r-$NiNb_2O_6$. The open symbols are experimental data and the solid curves are fitted results by $\sigma'(f) = \sigma_0 + \sigma_{ac} f^s$ relationship. The dashed arrow depicts the shift in the relaxation frequency of RX_L process. It can be illustrated that the higher frequency data becomes insufficient for fitting at higher temperatures.

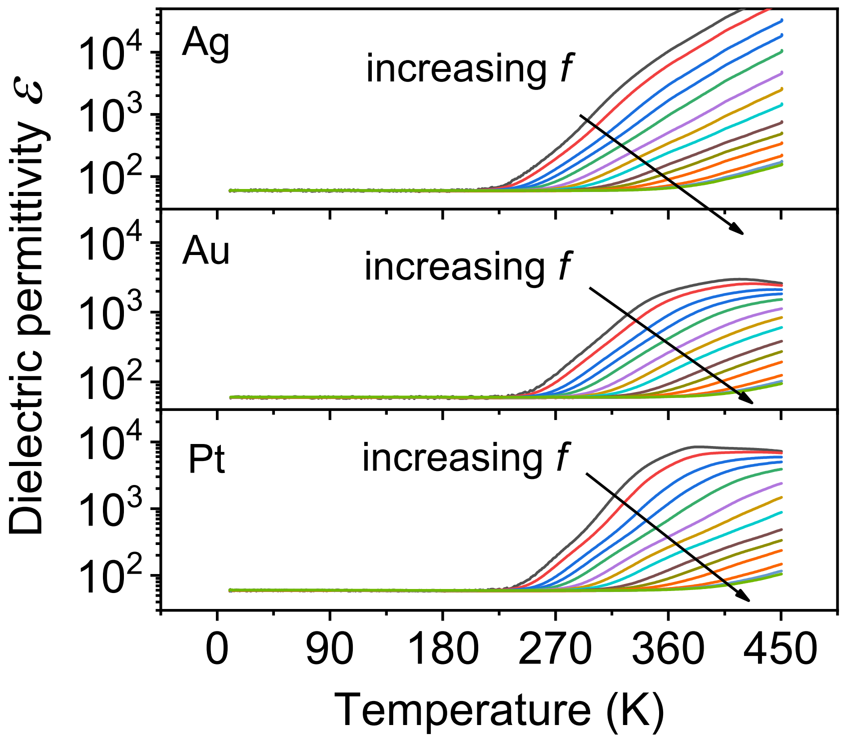

Figure S5 Temperature dependence of dielectric constant ε at 1000 Hz-1 MHz for r-$NiNb_2O_6$ coated with Ag, Au and Pt electrodes, respectively. The results shows that the polaron hopping induced colossal permittivity behavior (*i.e.* RX_H relaxation) which starts at ~220 K exists in all the samples with different electrode. However, the RX_L relaxation, which leads to the continuous rise in the low-frequency ε at $T >$ 360 K in Ag-coated sample, is weaker in Au- and Pt-coated samples, indicating that the RX_L is caused by Maxwell-Wagner effect.

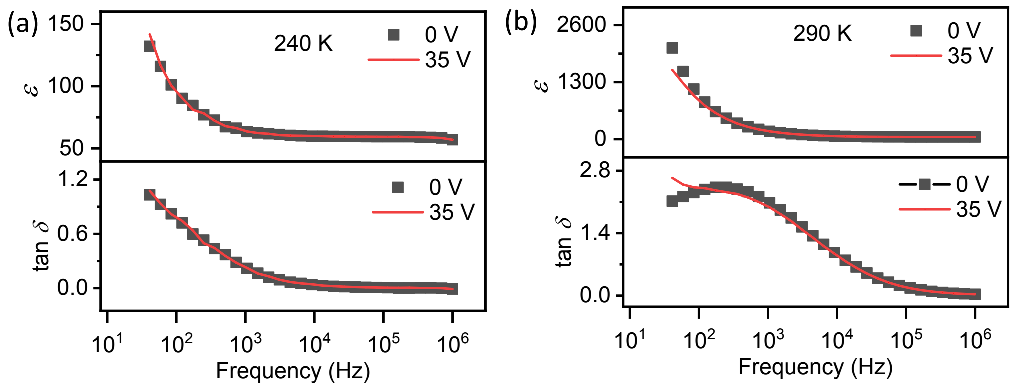

Figure S6 Frequency dependent dielectric spectra at 0 V and 35 V of applied bias at (a) 240 K, where the applied bias has no impact on dielectric properties, and (b) 290 K, where the dielectric permittivity at above 1000 Hz is unchanged under applied bias. The results indicate that the RX_H relaxation is not caused by the interfacial polarization.

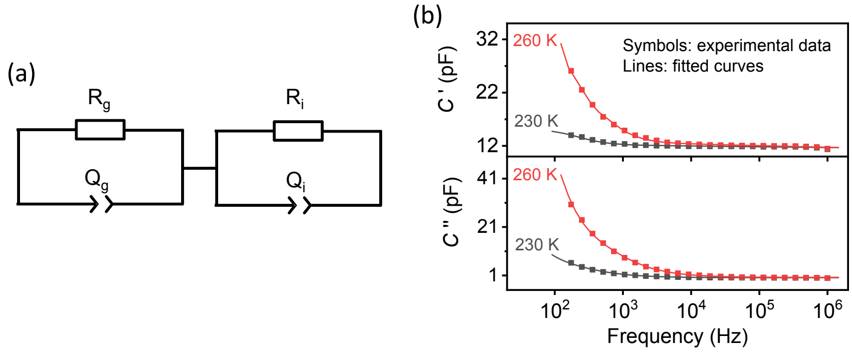

Figure S7 (a) The R_gQ_g-R_iQ_i circuit model used for fitting the dielectric spectra of r-$NiNb_2O_6$, where the R and Q represent the resistance and constant phase element, respectively; g and i represent the grain and interface, respectively. (b) The fitted results at selected temperatures. Note that when describing the interfacial polarization with the R_gQ_g-R_iQ_i model, the basic criteria of $R_g \ll R_i$ and $C_g \ll C_i$ should be fulfilled. However, the fitted results reveal the relationship of $R_g < R_i$ and $C_g > C_i$ in r-$NiNb_2O_6$ (**Table S1**), indicating that the interfacial polarization is not suitable for explaining the RX_H relaxation.

Table S1 Parameters of the circuit elements for the fitting in **Figure S6**. The equivalent capacitance of Q element is derived via $C_Q = (A \cdot R)^{\frac{1}{n}}/R$, where *A* and *n* are the parameters defining the impedance of Q element $Z_Q = 1/A(j\omega)^n$ and *R* is its parallel resistance.

T (K)	R_g(×10^{6}Ω)	A_{Qg}(×10^{-11})	n_{Qg}	C_{Qg} (×10^{-11}F)	R_i (×10^{6}Ω)	A_{Qi} (×10^{-11})	n_{Qi}	C_{Qi} (×10^{-11}F)
230	12.7	4.83	0.985	4.32	190	1.70	1	1.70
240	9.13	4.21	0.983	3.68	98.3	1.86	1	1.86
250	7.23	3.27	0.979	2.73	38.4	2.01	1	2.01
260	5.05	3.01	0.983	2.60	22.7	2.40	1	2.40

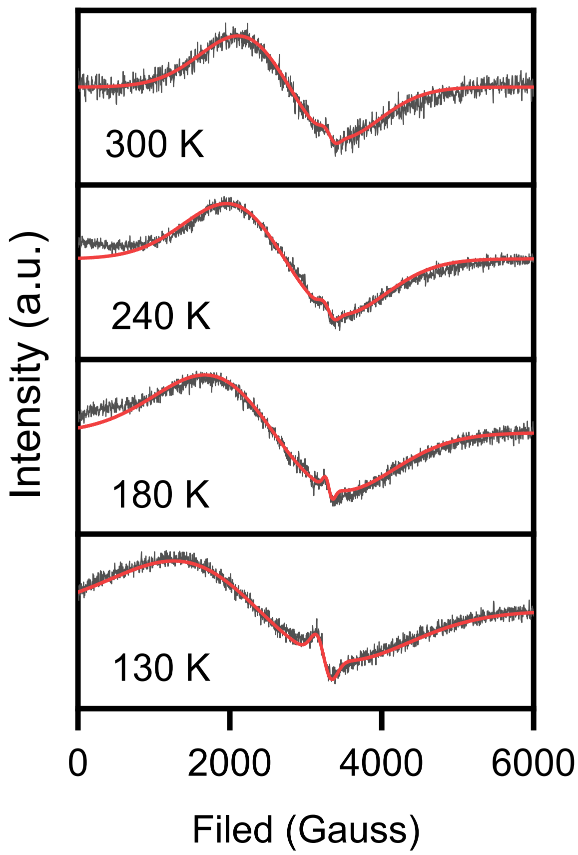

Figure S8 Temperature dependent EPR spectra for r-$NiNb_2O_6$. The black lines are experimental data. Each of the EPR lines (R1 and R2), and the red lines are fitted curves